Supplemental Material

Hypoxia-inducible factor activity promotes anti-tumor effector function and tissue residency by CD8$^+$ T cells

Ilkka Liikanen[1], Colette Lauhan[1], Sara Quon[1], Kyla Omulisik[1], Anthony T. Phan[1], Laura Barceló-Bartroli[1], Amir Ferry[1], John Goulding[1], Joyce Chen[2], James P. Scott-Browne[2], Jason T. Yustein[3], Nicole E. Scharping[1], Deborah A. Witherden[1], Ananda W. Goldrath[1*]

[1]Division of Biological Sciences, Section of Molecular Biology, University of California San Diego, San Diego, CA, 92161, USA.
[2]Division of Signaling and Gene Expression, La Jolla Institute for Immunology, La Jolla, CA, 92037, USA
[3]Texas Children's Cancer and Hematology Centers and The Faris D. Virani Ewing Sarcoma Center, Baylor College of Medicine, Houston, TX, 77030, USA.

*Correspondence: agoldrath@ucsd.edu

Supplemental Methods

Cancer Cell Lines

The B16.gp33, cell line was a gift from Dr. Alain Lamarre and is derived from C57BL/6 murine B16-F10 skin melanoma (1). B16.gp33 was cultured in DMEM supplemented with 10% fetal bovine serum, 1% penicillin and streptomycin, 1% L-glutamine, and 0.4 mg/mL of G-418 selective antibiotic (Geneticin; cat.# 10131019, Life Technologies). The MC38.gp33 cell line was generated from the commercially available C57BL/6 murine colon adenocarcinoma MC38 parental cell line (cat.# ENH204-FP, Kerafast) by stable transduction with a GFP-tagged pMIG retroviral vector expressing LCMV GP_{33-41} peptide (KAVYNFATC) and single cell-sorting to generate clones of MC38.gp33 cells. MC38.gp33 cells were cultured in DMEM supplemented with 10% fetal bovine serum, 1% penicillin and streptomycin and 1% L-glutamine. MSCV-puro containing a DNA fragment encoding human CD19 (hCD19) and the B16.hCD19 cell line were gifts from Dr. Anjana Rao (2) and the KRAS- and P-53-mutated murine rhabdomyosarcoma cell line (KMR) was a gift from Dr. Jason Yustein. The KMR cell line was established from murine tumors that developed in MyoD-Cre mice (3) crossed with LSL-$p53^{R172H}$ (NCI mouse repository) and LSL-K-Ras^{G12D} mice (NCI mouse repository). Tumors were comprehensively analyzed via histology and immunohistochemistry to confirm sarcoma diagnosis. Murine RMS tumors were isolated and KMR cell lines established directly from the tumors by disassociating the tumor using the Miltenyi gentle MACS Dissociator for enzymatic digestion. After digestion, cells were placed through a 70 μm cell strainer, washed and resuspended in media and plated into a 60 mm plate. The resulting rhabdomyosarcoma cell line was authenticated and confirmed to be of mouse origin and tested for evidence of cross-species contamination (human, rat, Chinese hamster, and African Green monkey). When 0.5-1 million KMR cells were placed orthotopically back into the gastrocnemius of C57BL/6 mice tumors were evident within 2-3 weeks. KMR.hCD19 cells were made by transducing with MSCV retroviral vector expressing hCD19 and then sorting cells for expression of hCD19. KMR.gp33 cells were made as described above for MC38.gp33. B16.hCD19, KMR.hCD19 and KMR.gp33 were cultured in DMEM supplemented with 10% fetal bovine serum, 1% penicillin and streptomycin, 1% 4-(2-hydroxyethyl)-1-piperazineethanesulfonic acid (HEPES), and 0.1% b-mercaptoethanol. Cell lines were treated for and/or confirmed mycoplasma free and authenticated in in vitro killing assays.

Donor T Cell Activation

Donor TCR-transgenic $CD8^+$ T cells were activated and expanded using the following protocol: First, spleens and lymph nodes were harvested from 6-12 week-old congenically-distinct mice for antigen-presenting cells, which were processed to single cell suspensions, irradiated with 2000 rad, incubated with 1 μM cognate peptide for 1.5 hours (KAVYNFATC for P14 or SIINFEKL for OT-I, Anaspec), washed and counted. Spleens and lymph nodes from 6-12 week-old congenically-distinct TCR-transgenic (P14 or OT-I) donor mice of appropriate genotype were harvested and processed to single-cell suspensions. Donor cells were plated at 1×10^6 donor cells together with 2.5×10^6 peptide-pulsed antigen-presenting cells. in 1.5 ml of T cell medium (RPMI-1640 supplemented with 10% FCS, 25 mM HEPES, 1% penicillin-streptomycin-glutamine and 55 μM β-mercaptoethanol) supplemented with 100 U/mL of recombinant human IL-2 (hIL-2, cat.# 200-02, Peprotech) and anti-mouse CD28 (1:1,000, clone 37.51; eBioscience). Donor cell cultures were split 1:2 after 48 hours and fresh T cell medium with hIL-2 was added. On day 4, donor cells were passaged and cultured further for in vitro assays or prepared for adoptive transfer. For generation of hCD19 CAR T cells, donor $CD8^+$ T cells were enriched from spleen and LN by negative selection. Single-cell suspensions were incubated with biotinylated antibodies to CD4 (GK1.5), Ter-119 (Ter119), NK1.1 (PK136), B220 (RA3-6B2), CD19 (1D3), and CD11b (M1/70; all from eBioscience) and then with streptavidin-labeled magnetic beads, followed by depletion on a MACS column. Enriched $CD8^+$ T cells were activated with anti-CD3 (1μg/ml clone 145-2C11; eBioscience) and anti-CD28 (1μg/ml) for 24 hours and transduced with retrovirus expressing anti-human CD19 CAR (a gift from Dr. Anjana Rao) (2) via centrifugation for 1 hour at 37°C and 2,000g. Cells were then incubated for 4 hours at 37°C prior to replacement of media with T cell medium with hIL-2 for 2-3 days. IL-2 was replaced daily while cells were expanded.

In Vitro Cytokine Sensitivity

Activated donor T cells were cultured for an additional 3 or 10 days in T- cell medium supplemented either with 100 U/mL of hIL-2 or with 10 ng/mL of recombinant murine IL-7 (cat.# 217-17, both from Peprotech), splitting the wells 1:2 every other day. For hypoxia studies, cells were split after the 4-day activation period into normoxic (21% ambient O_2) or hypoxic conditions (1% oxygen; Thermo Scientific-Hera Cell incubator), and cultured for additional 3 or 10 days with cytokines.

Immunofluorescence Microscopy

10 µm frozen sections were prepared on poly-L-lysine coated microscope slides (cat.# 067-CP, Cole-Parmer), dehydrated and temporarily stored flat in the dark at -20°C. Before staining, sections were thawed, rehydrated in 1× PBS and blocked for 20 minutes with 8% Fc receptor blocking medium (prepared in-house from hybridoma supernatant) diluted in universal blocking buffer containing 1% bovine serum albumin (cat.# A3294), 0.1% cold fish gelatin (cat.# G7041), 0.5% Triton X-100 (cat.# X100; all from Sigma-Aldrich) and 0.05% sodium azide in 10mM PBS, pH 7.2-7.4. Sections were stained for 2 hours at 4°C with Alexa Fluor® 647 anti-mouse CD8α (53-6.7, BioLegend), and anti-mouse hypoxyprobe-Dylight™549-MAb (4.3.11.3, Hypoxyprobe) prepared in universal blocking buffer. Slides were washed, counterstained with DAPI to detect nuclei (500 nM in PBS for 10 min, cat.# 422801, BioLegend), and mounted using SlowFade™ Gold Antifade Mountant (cat.# S36937, Invitrogen) under a glass coverslip (Fisherbrand). Immunofluorescence microscopy was performed using a Zeiss LSM 700 microscope and ZEN 2012 v.1.1.2.0 software (Carl Zeiss Microscopy). Image analysis was performed using ImageJ 1.52n software (National Institutes of Health). $CD8\alpha^+$ cells were counted by ImageJ and verified manually. For analysis of $CD8^+$ TIL localization, $CD8\alpha^+$ cells residing within or outside the hypoxic areas were counted.

Antibodies

The following antibodies were used for surface staining for flow cytometry (all from eBioscience unless otherwise specified): anti-CD8α (53-6.7), anti-CD45.1 (A20), anti-CD45.2 (104), anti-Vα2 (B20.1; BioLegend), anti-Vβ8.1/8.2 (KJ16-133), anti-Vβ5.1/5.2 (MR9-4), anti-CD8β (H35-17.2), anti-CD4 (RPA-T4; BD Horizon), anti-CD11a (M17/4), anti-CD25 (PC61.5), anti-CD27 (LG-7F9), anti-CD38 (90); anti-CD43 (1B11), anti-CD44 (IM7), anti-CD62L (MEL-14; BioLegend), anti-CD69 (H1.2F3), anti-CD95 (FasR;15A7), anti-CD101 (Moushi101), anti-CD103 (2E7), anti-CD122 (TM-b1), anti-CD127 (A7R34), anti-CD160 (7H1; BioLegend), anti-CD244 (2B4; 244F4), anti-CXCR3 (CXCR3-173), anti-GITR (DTA-1), anti-ICOS (ISA-3), anti-LAG-3 (C9B7W), anti-Ly-6C (HK1.4), anti-PD-1 (RMP1-14), anti-PD-L1 (MIH1), anti-TIM-3 (RMT3-23), anti-human CD19 (HIB19). The following antibodies were used for intracellular staining (all from eBioscience unless otherwise specified): anti-Bcl-2 (3F11 and 10C4); anti-Eomes (Dan11mag), anti-T-bet (4B10; BioLegend), anti-STAT5 (47/Stat5[pY694]; BD Phosflow); anti-Ki-67 (SolA15), anti-IFN-γ (XMG1.2), anti-TNF-α (MP6- XT22), anti-granzyme-B (GB12; Invitrogen); and anti-TCF1 (C63D9; Cell Signaling Technologies).

STAT-5A analysis

For analysis of phosphorylated STAT-5A, cultured cells were collected at indicated time points, washed twice and diluted to 1×10^7 cells/ml in serum-free RPMI 1640 and incubated for 30 min at 37°C in the presence of surface stain. The cells were then washed twice and incubated for a further 15 min at 37°C in PBS with or without 100 U/ml of IL-2 or 10 ng/ml of IL-7. Cells were immediately fixed for 20 min at 37°C using 1× Lyse/Fix Buffer (cat.# 558049, BD Phosflow), and permeabilized with Perm Buffer III (cat.# 558050, BD Phosflow) for 30 min on ice, washed twice in ice-cold Perm/Wash buffer (BD Biosciences) and stained with intracellular antibodies including anti-pSTAT5A (47/Stat5[pY694]; BD Phosflow) or Mouse IgG1 isotype (cat.# 555749; BD Pharmingen) for 30 min at room temperature, then analyzed immediately.

Cell Sorting and Ex Vivo Cytotoxicity Assays

Single-cell suspensions from isolated TIL and splenocytes were counted, stained with fluorochrome-conjugated viability dye for 10 min, washed and pre-incubated with Fc receptor blocking medium followed by surface staining in PBS supplemented with 2% bovine growth serum with appropriate antibodies. The following antibodies were used for surface staining for cell sorting (all from eBioscience): anti-CD8α (53-6.7), anti-CD45.1 (A20), anti-CD45.2 (104), anti-CD69 (H1.2F3) and anti-CD103 (2E7). Cells were then washed, kept on ice and resuspended in standard T-cell medium supplemented with 10% fetal bovine growth serum for the duration of the sorting. All sorting was performed on BD FACSAria Fusion instrument.

For ex vivo cytotoxicity assays: Sorted donor P14 TIL populations were diluted into equal concentration and added in triplicates on pre-washed 96-well culture plate wells with $1.5x10^5$ adherent target cancer cells, or on adjacent empty wells. For granzyme-B/Perforin-pathway blockade studies, soluble $MgCl_2$ (2 mM) and ethylene glycol tetraacetic acid (3 mM) were included in the culture medium (standard T-cell medium) for the duration of the killing assay. Assay plate(s) were incubated at 37.5°C for 6 hours. 50 µl of the supernatant was transferred into respective wells of a clear-bottom 96-well analysis plate(s), which was assessed for lactate dehydrogenase release using CytoTox 96® Non-Radioactive Cytotoxicity Assay kit (cat.# G1780, Promega) following manufacturer's instructions for Cell-Mediated Cytotoxicity Assay. Absorbance was recorded at 490 nm, background signal and volume correction control signal were subtracted from appropriate readings, and target cell lysis was calculated by formula: % cytotoxicity = (TIL experimental – TIL spontaneous – target spontaneous) / (target maximum – target spontaneous). After collecting the supernatant samples for cytotoxicity analysis, Protein Transport Inhibitor

Cocktail (1:500, Invitrogen) was added for 4 hours and cells were collected from assay wells for flow cytometry analysis.

Verification of in vivo antibody blocking

For staining of target-cell bound in vivo anti-CD103 antibody (rat IgG, clone M290, cat.# BE0026, BioXcell), isolated TIL and splenocytes were first blocked with 8% Fc receptor blocking medium (prepared from hybridoma supernatant) diluted in blocking solution containing 0.5% bovine serum albumin, 2% fetal calf serum, 2% normal mouse serum in PBS. Cells were then stained with biotinylated anti-rat IgG (cat.# 112-065-167, Jackson Immunoresearch) in the blocking buffer at 4°C for 30 minutes, washed twice and stained for 30 minutes with PE-Cy7-labeled streptavidin (eBioscience) together with other fluorochrome-conjugated antibodies at 4°C for 30 minutes. All stained cells were analyzed by using LSRFortessa X-20 (BD Biosciences) and FlowJo software v.10.1 (BD).

Quantitative Reverse-Transcription Polymerase Chain Reaction

To confirm *Vhl* deletion in intratumoral ER-Cre^{+} P14 cells following in vivo tamoxifen treatment on days 3-7 post-transfer, total RNA was extracted from ER-Cre^{-} and ER-Cre^{+} P14 TIL populations sorted from the same tumor on day 9 post-transfer by using TRIzol (cat.# 15596026, Invitrogen). cDNA was synthesized by using SuperScript™ II Reverse Transcriptase (cat.#18064022, Invitrogen) according to the manufacturer's instructions. For quantitative polymerase chain reaction, cDNA was quantitatively amplified by using Brilliant II Syber Green master mix kit (cat.# 600828, Agilent Technologies). *Vhl* transcript levels were normalized to the housekeeping gene *Hprt*. The following primers were used:

Vhl forward, 5′-CTAGGCACCGAGCTTAGAGGTTTGCG-3′ and

Vhl reverse, 5′-CTGACTTCCACTGATGCTTGTCACAG-3′;

Hprt forward, 5′-GGCCAGACTTTGTTGGATTT-3′, and

Hprt reverse: 5′-CAACTTGCGCTCATCTTAGG-3′.

Gene Signature Analysis

For comparative analysis of gene signatures and GSEA, the control CD8^{+} T cell subsets of *bona fide* T_{RM}, TE, LLE, T_{EM} were generated in mouse infection models at memory time points as follows:

The core tissue-resident memory $CD8^+$ T cell (T_{RM}) signature was previously generated by integrating differential expression data (>1.5 fold change) comparing T_{RM} cells residing in gut, kidney, skin, lung and brain to their respective circulating memory (or T_{CM}) cells at memory time points of various mouse infection models (4). The $CD8^+$ T cell exhaustion signature is derived from LCMV Clone 13 infected mice reported in (5), and the terminal and progenitor exhaustion signatures are derived from TILs in B16-OVA tumor bearing mice (6). The terminal effector (TE) signature is derived from previously generated data by examining differentially expressed genes between TE and MP samples (> 2 fold change and <0.01 p-value) (4). The long-lived effector (LLE) cell, effector-memory T cell (T_{EM}), and central-memory T cell (T_{CM}) signatures were generated from LCMV Armstrong infected mice (7). The LLE and T_{EM} signatures were made by contrasting with T_{CM} (> 2 fold change).

Supplemental References

1. Fidler IJ. Selection of successive tumour lines for metastasis. *Nat New Biol.* 1973;242(118):148-9.
2. Chen J, Lopez-Moyado IF, Seo H, Lio CJ, Hempleman LJ, Sekiya T, et al. NR4A transcription factors limit CAR T cell function in solid tumours. *Nature.* 2019;567(7749):530-4.
3. Chen JC, Mortimer J, Marley J, and Goldhamer DJ. MyoD-cre transgenic mice: a model for conditional mutagenesis and lineage tracing of skeletal muscle. *Genesis.* 2005;41(3):116-21.
4. Milner JJ, Toma C, Yu B, Zhang K, Omilusik K, Phan AT, et al. Runx3 programs CD8(+) T cell residency in non-lymphoid tissues and tumours. *Nature.* 2017;552(7684):253-7.
5. Bengsch B, Ohtani T, Khan O, Setty M, Manne S, O'Brien S, et al. Epigenomic-Guided Mass Cytometry Profiling Reveals Disease-Specific Features of Exhausted CD8 T Cells. *Immunity.* 2018;48(5):1029-45 e5.
6. Miller BC, Sen DR, Al Abosy R, Bi K, Virkud YV, LaFleur MW, et al. Subsets of exhausted CD8(+) T cells differentially mediate tumor control and respond to checkpoint blockade. *Nat Immunol.* 2019;20(3):326-36.
7. Milner JJ, Nguyen H, Omilusik K, Reina-Campos M, Tsai M, Toma C, et al. Delineation of a molecularly distinct terminally differentiated memory CD8 T cell population. *Proc Natl Acad Sci U S A.* 2020;117(41):25667-78.

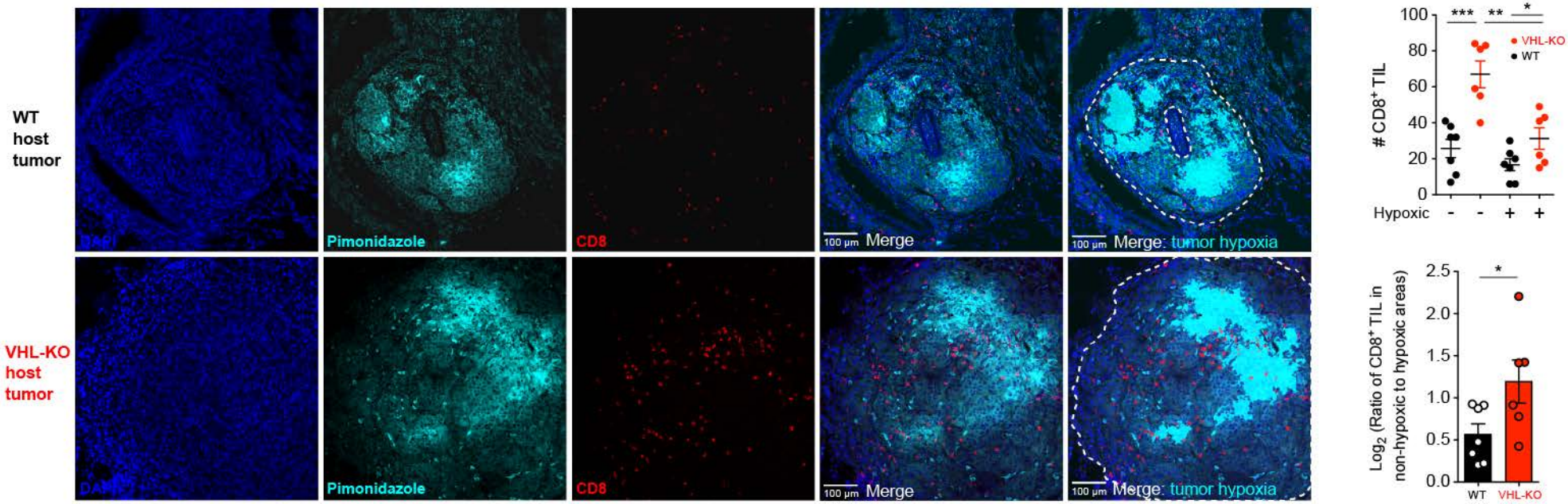

Liikanen et al. Fig. S1: Polyclonal VHL-deficient CD8+ TIL are more prevalent in metastatic melanoma lesions in the lungs and are localized to less-hypoxic regions of tumors

Supplemental Figure 1: Polyclonal CD8$^+$ T cells VHL-deficient TIL are more prevalent in metastatic melanoma lesions in the lungs and are localized to less-hypoxic regions of tumors.

Representative micrograph images of a metastatic B16.gp33 lesion in the lung parenchyma of a WT (top row) and a VHL-KO mouse (bottom row) showing DAPI (left), Hypoxyprobe (middle) and CD8a (right) staining. For analysis of CD8$^+$ TIL localization, greater than the mean fluorescence intensity of control pimonidazole emission was highlighted (cyan color, 5th image) and overlaid with the merged image (4th image). Dotted lines indicate tumor lesion borders. Absolute number of CD8$^+$ TIL residing within each compartment (top far right) and Log_2-transformed ratio of TIL localization in non-hypoxic to hypoxic tumor areas are shown (bottom far right).

Data are pooled from 2 independent experiments with 3-6 mice per group. Symbols represent individual tumors. Bars represent mean ± SEM of replicate measurements. *p < 0.05, **p < 0.01, ***p < 0.001, ****p < 0.0001 (Student's *t*-test).

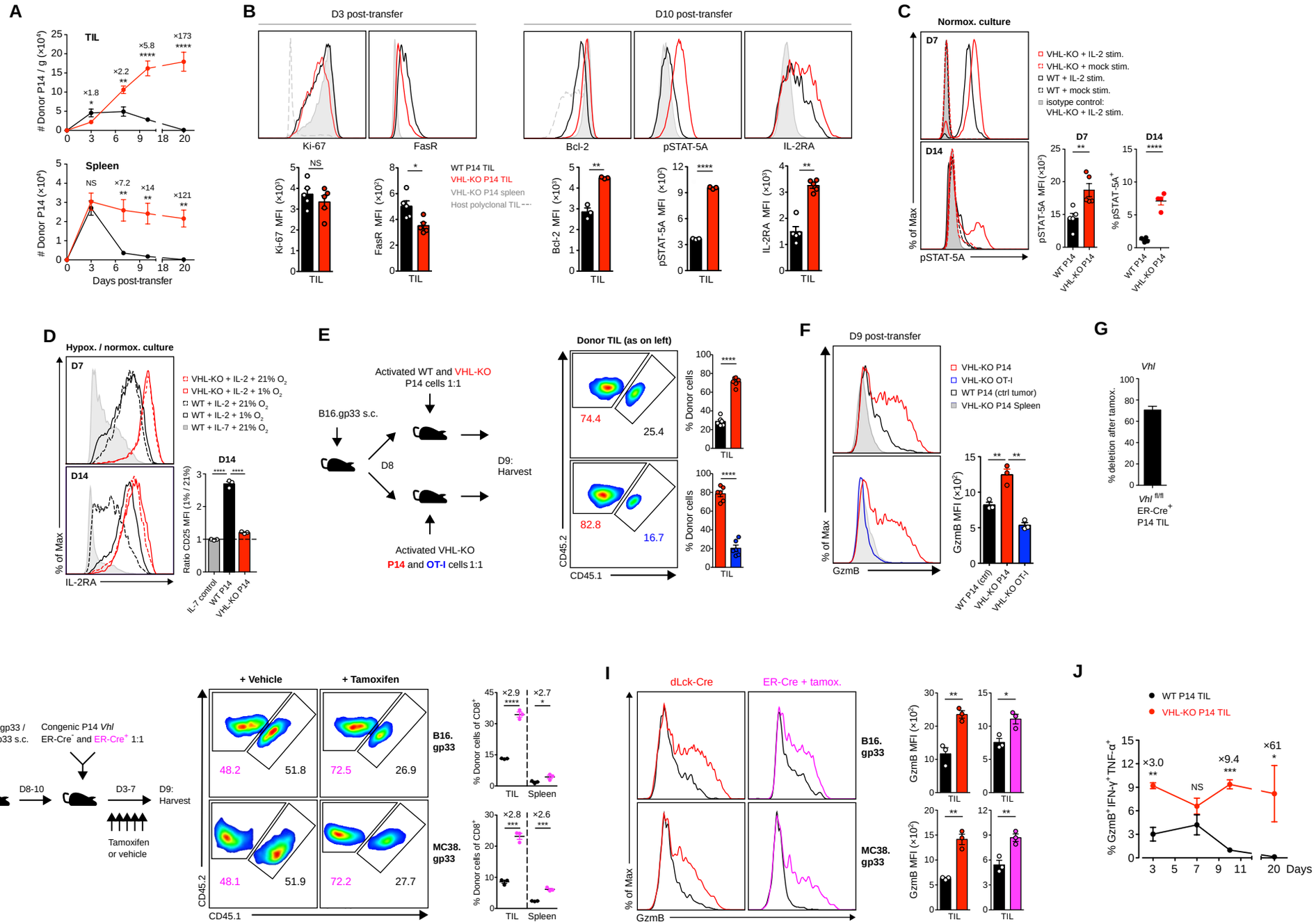

Liikanen et al. Fig. S2: VHL-deficient TIL display enhanced survival, cytokine sensitivity, accumulation and Granzyme B expression that is dependent on antigen-recognition and independent of VHL status during activation

Supplemental Figure 2: VHL-deficient TIL display enhanced survival, cytokine sensitivity, accumulation and granzyme-B expression that is dependent on antigen-recognition and independent of VHL status during activation.

(**A**) Weight-adjusted cell numbers of co-transferred WT and VHL-KO P14 TIL (top) and spleens (bottom) at indicated time points following transfer at a 1:1 ratio into mice bearing subcutaneous B16.gp33 tumors.

(B) Representative flow cytometry histograms (top panels) of Ki-67 Fas (FasR) expression on donor TIL on day 3 following transfer, and IL-2Ra (CD25), phosphorylated STAT-5A (pSTAT-5A), and Bcl-2 expression on day 10. Bottom panels show comparisons of mean fluorescence intensities between donor P14 TIL populations.

(C) Representative flow cytometry histograms (left panels) of phosphorylated STAT-5A expression for in vitro activated WT and VHL-KO P14 cells after 7 days (top) or 14 days (bottom) of culture. Quantification of pSTAT-5A signal on a per cell basis on day 7 (bottom middle) and by frequency on day 14 (bottom right).

(**D**) IL-2Ra expression by P14 cells activated and cultured for 4 days followed by either normoxic (21% O_2) or hypoxic (1% O_2) conditions for 3 (top) or 10 (bottom) days. Culture in IL-7 was used as a negative control, while VHL-KO P14 cells with constitutively active HIF signaling acted as a positive control. Impact of hypoxia on retained IL-2 receptor expression on day 14 is presented as the ratio of mean fluorescence intensities between hypoxic and normoxic culture conditions.

(**E**) Representative flow cytometry of donor TIL populations and quantification of their frequencies 9 days after 1:1 transfer of CD45 congenically distinct WT and VHL-KO P14 cells (top) or VHL-KO P14 and OT-I cells (bottom) into B16.gp33 tumor-bearing mice.

(**F**) Representative histograms of granzyme-B expression (left) and quantification of mean fluorescence intensities (right) of donor TIL populations in (F).

(**G**) In vivo deletion efficiency of *VHL* gene in donor *Vhl*$^{fl/fl}$ ER-Cre^{+} P14 TIL, sorted by congenic markers from B16.gp33 tumors on day 9 after co-transfer and tamoxifen treatment on days 3 and 7.

(**H**) Representative flow cytometry of donor P14 TIL populations 9 days after 1:1 transfer of *Vhl*$^{fl/fl}$ ER-Cre^{-} and *Vhl*$^{fl/fl}$ ER-Cre^{+} P14 cells and after vehicle (left) or tamoxifen (right) treatment on days 3 and 7. Frequency of donor cells in tumors and spleen of tamoxifen treated mice are shown on the far right.

(**I**) Representative histograms of Granzyme-B expression in co-transferred donor P14 TIL populations recovered from B16.gp33 (top row) and MC38.gp33 tumors (bottom row) in two conditional knock-out models: Deletion prior to activation as in (A) (red) and deletion after activation and adoptive co-transfer by tamoxifen treatment as in (H) (magenta). Comparisons of respective mean fluorescence intensities are shown on the right.

(**J**) Frequency of granzyme B^{+}IFN-γ $^{+}$TNF-α $^{+}$ triple positive donor TIL recovered over time from B16.gp33 tumor bearing animals following 1:1 co-transfer of WT and VHL-KO P14 cells TIL were re-stimulated with cognate gp33 peptide and granzyme-B, IFN-γ and TNF-α measure by flow cytometry.

Data are pooled in (A) and representative in other panels of 2 or more independent experiments with 3 or more mice per genotype and assay condition. Co-transfer experiments were performed for time points 3, 7, 10 and day 20 post-transfer in (A, B and E). For day 20, corresponding phenotype was observed for co-transferred and single-transferred animals, but the single transfer model presented in figure 1A was used in (K) to allow sufficient numbers of wild-type P14 TIL for functional analyses. Symbols represent individual mice in (B, F-H and J), individual donor cultures in (C-D) and mean in (A, E, I and K). Mean fold increase in frequency (E, H and K) and in weight-adjusted count (A) between groups are provided where appropriate. Bars, line charts and error represent mean ± SEM of replicate measurements. NS, not significant, *$p < 0.05$, **$p < 0.01$, ***$p < 0.001$, ****$p < 0.0001$ (Student's *t*-test).

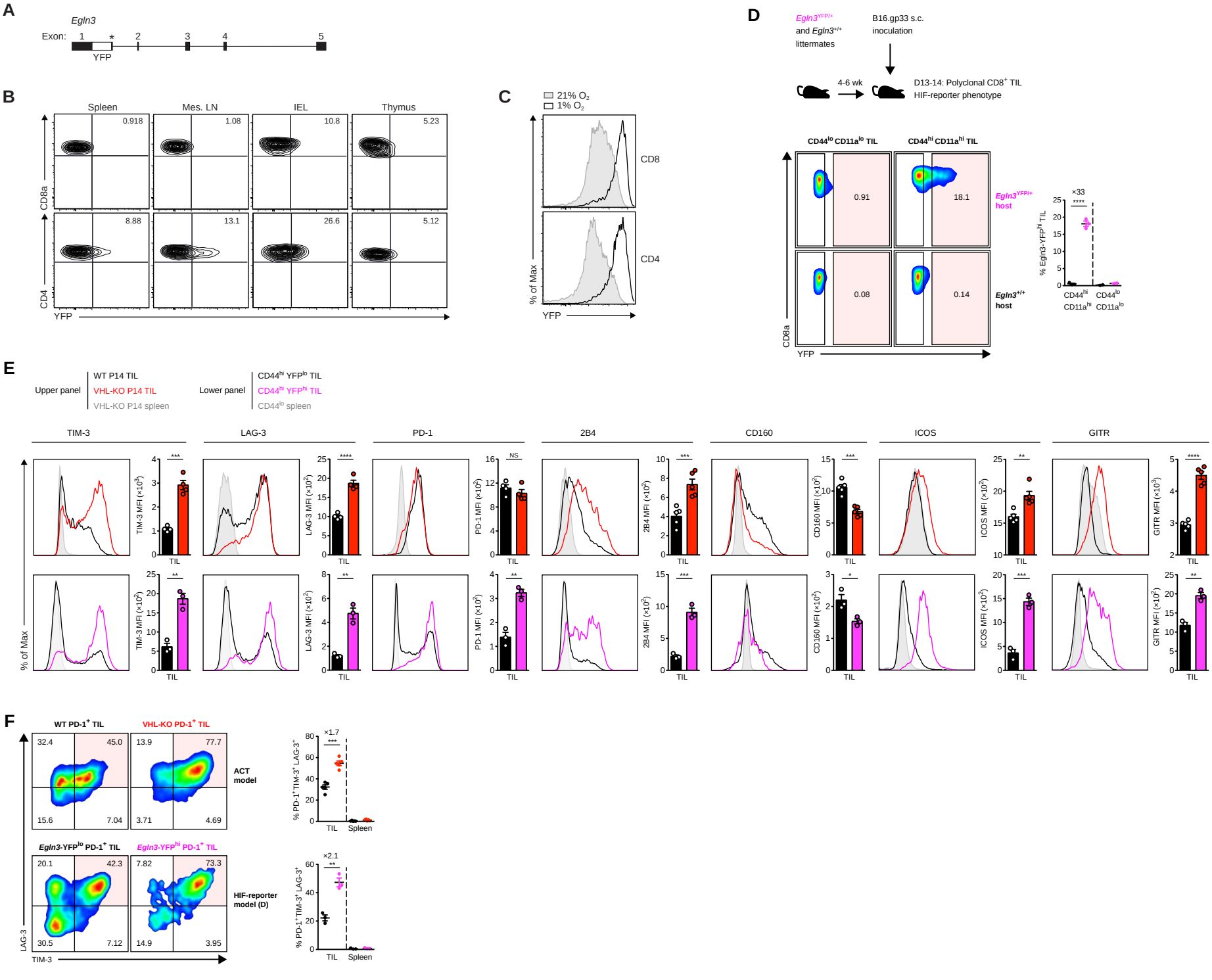

Liikanen et al. Fig. S3: HIF activity in polyclonal CD8+ TIL correlates with activated phenotype of VHL-KO P14 TIL, characterized by expression of both co-stimulatory and exhaustion-associated markers

Supplemental Figure 3: HIF activity in polyclonal CD8$^+$ TIL correlates with activated phenotype of VHL-KO P14 TIL, characterized by expression of both co-stimulatory and exhaustion-associated markers.

(**A**) To assess the role of HIF transcriptional activity on T cell responses in vivo and to identify cells with recent HIF activity, the turboYFP sequence was inserted following the first exon of the HIF1α and HIF2α target gene *Egln3*. The YFP insert introduces a stop codon (*) disrupting the *Egln3* gene, and therefore subsequent studies were performed with heterozygous animals (*Egln3*$^{YFP/+}$).

(**B**) Representative flow cytometry analysis of YFP signal in CD8$^+$ (top row) and CD4$^+$ (bottom row) T cells isolated from indicated organs of a naive adult *Egln3*$^{YFP/+}$ mouse.

(**C**) Representative histograms of YFP signal in activated CD8$^+$ (top) and CD4$^+$ (bottom) T cells after incubation under indicated O_2 tension.

(**D**) Representative flow cytometry of YFP signal in TIL from polyclonal *Egln3*$^{YFP/+}$ reporter (magenta) and *Egln3*$^{+/+}$ control (black) mice 13-14 days following inoculation with B16.gp33 tumor cells. Cells were gated on CD8$^+$ and CD44^{hi}CD11a^{hi} or CD44^{lo}CD11a^{lo} and YFP plotted versus CD8 expression. Frequency of YFP$^+$ cells is quantified on the right.

(**E**) Flow cytometry and quantification of the indicated markers on co-transferred donor WT (black) versus VHL-KO (red) P14 TIL populations recovered on days 10-11 post-transfer (top row), or polyclonal CD44-high CD8$^+$ TIL harboring low (black) *versus* high YFP signal (magenta) recovered from *Egln3*$^{YFP/+}$ mice on days 13-14 after tumor inoculation (bottom row).

(**F**) Co-expression of key exhaustion-associated markers PD-1, TIM-3 and LAG-3 on B16.gp33 donor TIL at day 10-11 after co-transfer of VHL-KO P14 and WT P14 cells (top row, ACT model) and on polyclonal CD8$^+$ TIL of *Egln3*$^{YFP/+}$ reporter mice on day 13-14 after tumor inoculation (bottom row, HIF-reporter model). Representative flow cytometry analysis on the left shows co-expression of TIM-3 and LAG-3 (highlighted quadrant) gated on PD-1-high CD44-high CD8$^+$ TIL, and the frequency of triple-positive (PD-1$^+$TIM-3$^+$LAG-3$^+$) cells within each population are quantitated on the right.

Data are representative of 2 or more independent experiments with 3 or more mice per genotype. Symbols represent individual mice. Mean fold increase in frequency (D, F) are provided where appropriate. Bars and error represent mean ± SEM of replicate measurements. NS, not significant, *$p < 0.05$, **$p < 0.01$, ***$p < 0.001$, ****$p < 0.0001$ (Student's *t*-test). Mes. LN,

mesenteric lymph node; IEL, intraepithelial lymphocytes (of mouse small intestine); ACT, adoptive cell transfer.

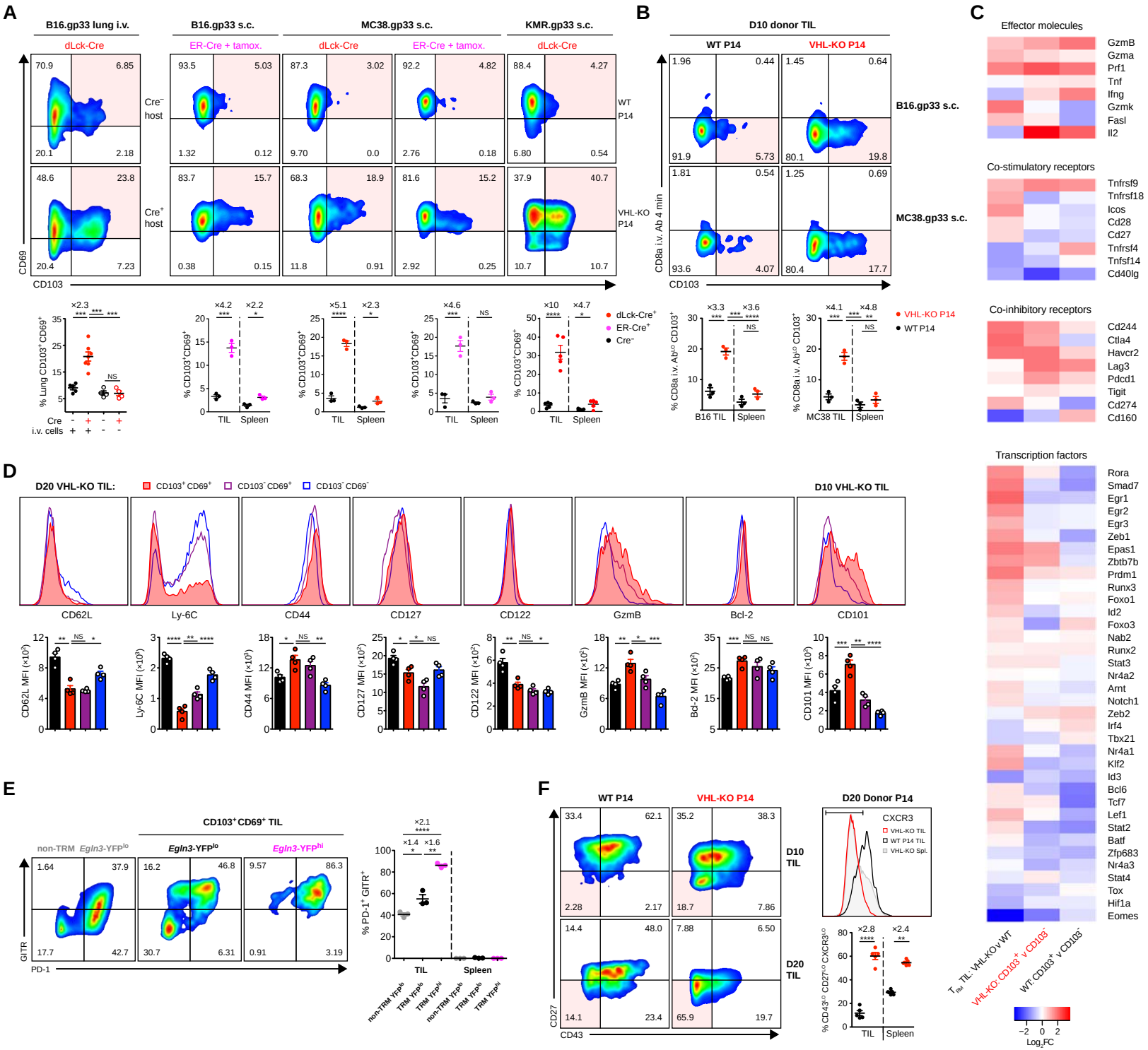

Liikanen et al. Fig. S4: Accumulation of CD103+CD69+ TIL subset irrespective of the timing of *Vhl* deletion and a subset of long-lived effector cells

Supplemental Figure 4: Accumulation of CD103$^+$CD69$^+$ TIL subset irrespective of the timing of *Vhl* deletion and a subset of long-lived effector cells

(**A**) Representative flow cytometry plots of TIL (top panels) and quantification of indicated subsets in tumors and spleen (bottom panels) for WT and VHL-KO CD8$^+$ TIL on day 21 in the polyclonal B16.gp33 lung metastasis model (far left column), or on day 15 in the adoptive transfer model. For adoptive transfer models, VHL was deleted either prior to (dLcK-Cre, red) or after (ER-Cre, magenta) co-transfer of Cre$^-$ or Cre$^+$ P14 cells into mice bearing B16.gp33, MC38.gp33 or KMR.gp33 tumors as indicated. For the polyclonal lung metastasis model, quantification of CD103$^+$CD69$^+$ cells in control mice without tumor challenge is also shown (graph on far left).

(**B**) Representative flow cytometry plots showing i.v. anti-CD8a staining that marks circulatory P14 cells within tumors (y-axis), versus CD103 expression in B16.gp33 and MC38.gp33 tumors. Highlighted quadrants represent i.v. CD8a-negative subset indicating T_{RM}-like donor P14 TIL, and bottom panels show the frequency of these cells in indicated tissues and tumor models after co-transfer.

(**C**) Transcriptional profiles of indicated P14 TIL subsets on day 7 after co-transfer of congenically distinct littermate donor WT and VHL-KO P14 cells sorted from B16.gp33 tumors as in Figure 4. Left columns compare T_{RM}-like TIL subsets between the donor P14 populations, middle and right columns compare T_{RM}-like TIL to non-T_{RM} TIL within a donor population.

(**D**) Representative histograms (top panels) and MFI (bottom panels) of expression of indicated markers for CD103$^+$CD69$^+$ (red), CD103$^-$CD69$^+$ (purple) and CD103$^-$CD69$^-$ (blue) subsets of VHL-KO P14 TIL on day 20 or day 10 (CD101) after transfer. MFI on co-transferred bulk WT P14 TIL (black bars) are also shown in the bottom panels.

(**E**) Representative flow cytometry analysis and quantification of PD-1 and GITR expression on YFP-low (black) *versus* YFP-high (magenta) subsets of CD44-high CD8$^+$ TIL gated on CD69$^+$CD103$^+$ following challenge of polyclonal *Egln3*$^{YFP/+}$ reporter mice with B16.gp33 melanoma cells. Non T_{RM}-like CD69$^-$CD103$^-$ CD8$^+$ TIL are shown in gray. Frequency of each population is shown. Splenocytes with universally low expression of exhaustion-activation markers were used as negative controls.

(**F**) Representative flow cytometry plots (left) of CD43 and CD27 expression on donor P14 TIL 10 days (top panels) and 20 days (bottom panels) after co-transfer in the B16.gp33 tumor model. Expression of CXCR3 on day 20 post-transfer (top right, representative histogram). Frequency of

the long-lived effector-like CXCR3^{-}CD43^{-}CD27^{-} TIL subset and splenocytes on day 20 are quantitated on the bottom right.

Data are representative of 2 or more independent experiments with 3 or more mice per genotype. For RNA sequencing data in (C), 2 biological replicates of 5 co-transferred mice each were prepared and analyzed in parallel, which are also used for analysis Figure 4. Symbols represent individual mice. Mean fold increase in frequency (A, B, E and F) between groups are provided where appropriate. Bars and error represent mean ± SEM of replicate measurements. NS, not significant, *p < 0.05, **p < 0.01, ***p < 0.001, ****p < 0.0001 (Student's *t*-test).

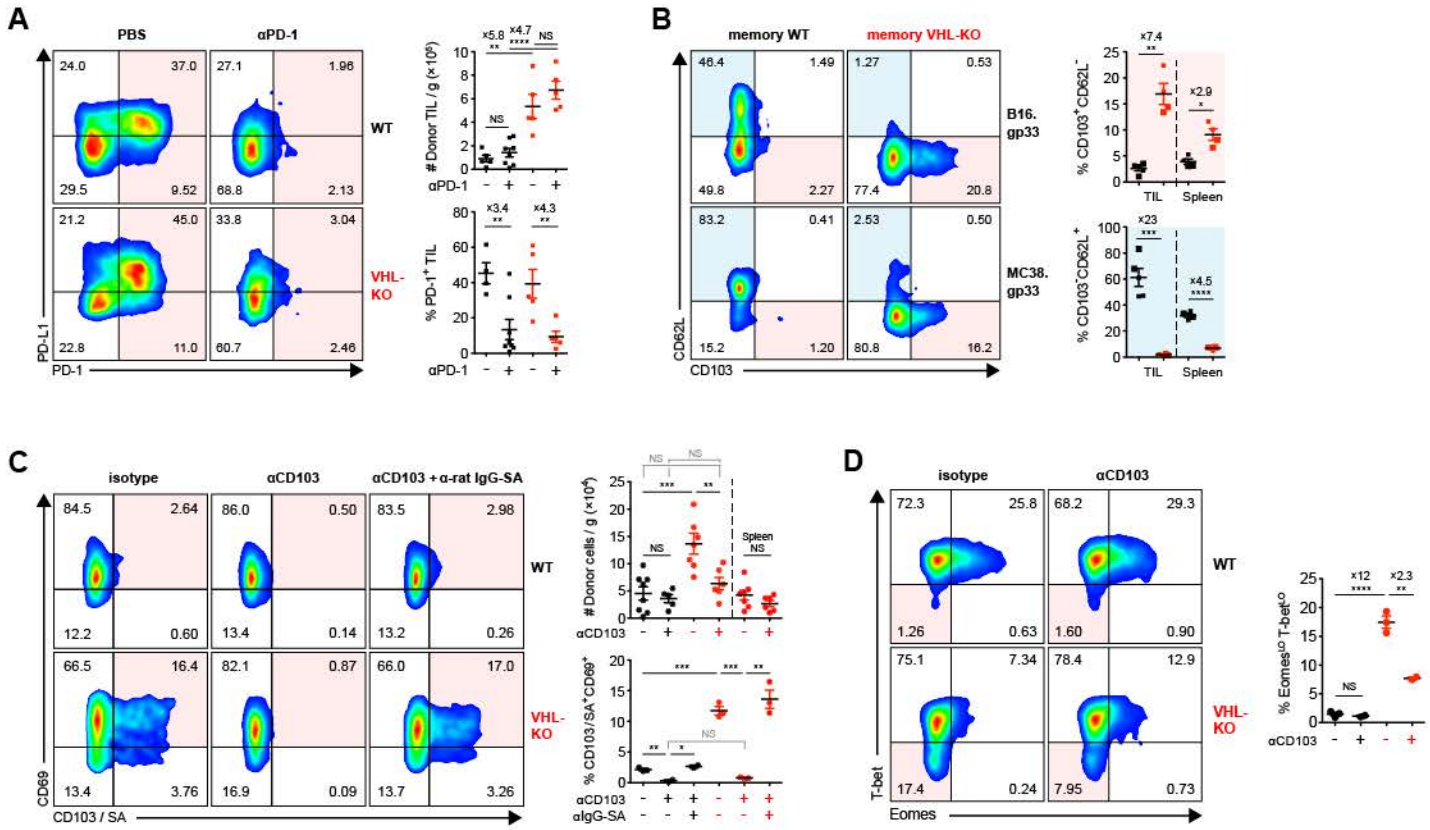

Liikanen et al. Fig. S5: Antibodies against PD-1 and CD103 effectively block *in vivo*

Supplemental Figure 5: Antibodies against PD-1 and CD103 effectively block in vivo

(**A**) Quantification of donor P14 TIL in tumors after in vivo PBS (-) or anti-PD-1 treatment (+) at end point of experiments in Figure 5A (top right). Representative flow cytometry of PD-1 and PD-L1 expression on indicated donor P14 TIL after in vivo PBS (left column) or anti-PD-1 treatment (right column). which are quantitated by frequency on bottom right.

(**B**) Representative flow cytometry in B16.gp33 and MC38.gp33 tumor models of CD62L (light blue) or CD103 (light red) expression in memory P14 TIL subsets and quantified on the right. Circle and square symbols indicate memory P14 cells recovered from animals re-challenged with B16.gp33 and MC38.gp33, respectively.

(**C**) Representative flow cytometry panel shows CD103 and CD69 T_{RM} marker expression on indicated donor P14 TIL after isotype (left column) or αCD103 treatment (middle column), and the visualization of in vivo bound αCD103 on the latter cells by SA signal (right column; same cells as middle). Assessment of CD103 expression to blockade efficiency is quantified on the bottom right, where frequency of $CD69^{+}SA^{+}$ is used instead of $CD69^{+}CD103^{+}$ where indicated.

(**D**) Representative flow cytometry of T-bet and Eomes expression on co-transferred donor P14 TIL populations after in vivo anti-CD103 or isotype treatment. Cells were collected for intracellular analysis from triplicate wells after CTL assay. Frequency of $Eomes^{lo}$ $T\text{-}bet^{lo}$ donor cells for each group is quantitated on the right.

Data are representative of 2 or more independent experiments with three or more mice per genotype and treatment condition. Symbols represent individual mice. Bars and error represent mean ± SEM of replicate measurements. NS, not significant, *$p < 0.05$, **$p < 0.01$, ***$p < 0.001$, ****$p < 0.0001$ (Student's t-test).

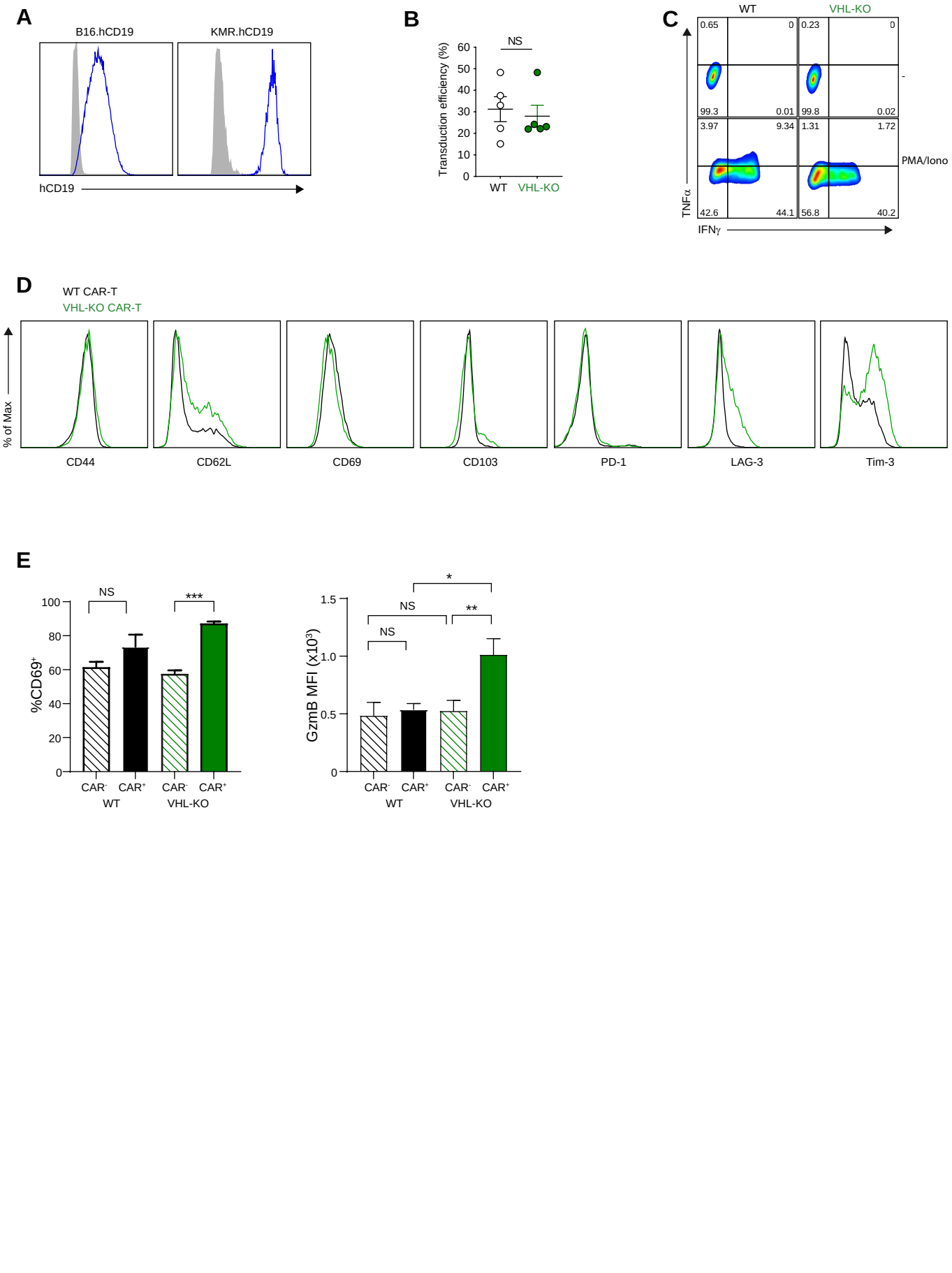
A
B16.hCD19
KMR.hCD19
hCD19
B
NS
Transduction efficiency (%)
60
50
40
30
20
10
0
WT
VHL-KO
C
WT
VHL-KO
0.65
0
0.23
0
99.3
0.01
99.8
0.02
3.97
9.34
1.31
1.72
42.6
44.1
56.8
40.2
-
PMA/Iono
TNFα
IFNγ
D
WT CAR-T
VHL-KO CAR-T
% of Max
CD44
CD62L
CD69
CD103
PD-1
LAG-3
Tim-3
E
NS
***
%CD69+
100
80
60
40
20
0
CAR-
CAR+
CAR-
CAR+
WT
VHL-KO
*
NS
**
NS
GzmB MFI (x10³)
1.5
1.0
0.5
0
CAR-
CAR+
CAR-
CAR+
WT
VHL-KO

Supplemental Figure 6: VHL-deficient CD8$^+$ CAR T cells show enhanced anti-tumor activity

(**A**) Representative flow cytometry plots of CD19 expression on transduced B16 and KMR tumor cell lines.

(**B**) Transduction efficiency of anti-human CD19 CAR into WT and VHL-KO CD8 T cells.

(**C**) IFNg and TNFa production by WT (left) and VHL-KO (right) following in vitro stimulation with PMA and ionomycin (bottom) or left unstimulated (top).

(**D**) Representative FACS plots of indicated surface marker expression on WT and VHL-KO CAR-T cells prior to adoptive transfer.

(**E**) CD69 and granzyme B expression on WT and VHL-KO CAR$^-$ (striped bars) and CAR$^+$ (solid bars) CD8 TIL 8 days after co-transfer into B16.hCD19 tumor bearing mice.

Bars and error represent mean ± SEM of replicate measurements. NS, not significant, *p < 0.05, **p < 0.01, ***p < 0.001 (Student's t-test).